Augmenting Experimental Gastric Cancer Activity of Irinotecan through Liposomal Formulation and Antiangiogenic Combination Therapy

Niranjan Awasthi[1,2], Margaret A. Schwarz[2,3], Changhua Zhang[4], Stephan G. Klinz[5], Florence Meyer-Losic[6], Benjamin Beaufils[6], Arunthathi Thiagalingam[5], and Roderich E. Schwarz[1,2,7]

ABSTRACT

Gastric adenocarcinoma (GAC) is the third most common cause of cancer-related deaths worldwide. Combination chemotherapy remains the standard treatment for advanced GAC. Liposomal irinotecan (nal-IRI) has improved pharmacokinetics (PK) and drug biodistribution compared with irinotecan (IRI, CPT-11). Angiogenesis plays a crucial role in the progression and metastasis of GAC. We evaluated the antitumor efficacy of nal-IRI in combination with novel antiangiogenic agents in GAC mouse models. Animal survival studies were performed in peritoneal dissemination xenografts. Tumor growth and PK studies were performed in subcutaneous xenografts. Compared with controls, extension in animal survival by nal-IRI and IRI was >156% and >94%, respectively. The addition of nintedanib or DC101 extended nal-IRI response by 13% and 15%, and IRI response by 37% and 31% (MKN-45 xenografts); nal-IRI response by 11% and 3%, and IRI response by 16% and 40% (KATO-III xenografts). Retardation of tumor growth was greater with nal-IRI (92%) than IRI (71%). Nintedanib and DC101 addition tend to augment nal-IRI or IRI response in this model. The addition of antiangiogenic agents enhanced tumor cell proliferation inhibition effects of nal-IRI or IRI. The tumor vasculature was decreased by nintedanib (65%) and DC101 (58%), while nal-IRI and IRI alone showed no effect. PK characterization in GAC xenografts demonstrated that compared with IRI, nal-IRI treatment groups had higher retention, circulation time, and tumor levels of CPT-11 and its active metabolite SN-38. These findings indicate that nal-IRI, alone and in combination with antiangiogenic agents, has the potential for improving clinical GAC therapy.

Introduction

Gastric adenocarcinoma (GAC) remains the third leading cause of cancer mortality worldwide (1). Combination chemotherapy regimens are the standard treatment for patients with GAC and lead to a modest improvement in survival, but median survival time remains less than a year (2–4). A triple chemotherapy regimen with docetaxel, oxaliplatin and 5-FU (FLOT) demonstrated superior clinical efficacy and became the standard perioperative treatment for patients with gastric cancer (5). For second-line therapy, cytotoxic agents such as irinotecan and taxanes are known to improve the prognosis for patients with GAC. In addition, some molecular targeted agents such as trastuzumab, a HER2 antibody, and ramucirumab, a VEGFR2 antibody, are also approved for advanced GAC therapy as monotherapy or in combination with chemotherapy (6). On the basis of the low response rates of these intensive therapies and the development of chemoresistance and relapse (7), there is an urgent need for novel therapeutic strategies that can improve clinical GAC therapy.

Irinotecan (IRI, CPT-11) and its active metabolite SN-38 bind reversibly to the topoisomerase I-DNA complex, thus preventing religation of single-strand DNA breaks and inducing cancer cell death (8). Previous studies reported the effectiveness of irinotecan against advanced GAC as monotherapy (9) and in combination with other chemotherapy drugs (10, 11). Several phase II studies demonstrated the second-line activity of irinotecan with or without fluoropyrimidines in patients with advanced GAC (12–14). The clinical activity of irinotecan has been limited by some of its chemical, pharmacokinetic (PK), and tolerability properties such as the conversion of its active lactone form to inactive carboxylate form at physiological pH (15, 16), rapid elimination of the drug (17, 18), and drug-induced diarrhea (19). Liposomal irinotecan (nal-IRI) is an intravenous liposomal formulation that encapsulates the topoisomerase I inhibitor irinotecan in a lipid bilayer vesicle (long-circulating liposomes). Liposomal encapsulation of irinotecan has shown improved circulating PK properties and increased tumor residence of both CPT-11 and SN-38 as compared with IRI (20, 21). Nal-IRI demonstrated promising antitumor efficacy and improved safety profile in preclinical studies (20–23). Nal-IRI also showed encouraging response as second-line therapy in several phase II studies including patients with gemcitabine-refractory advanced pancreatic cancer, patients with gemcitabine plus cisplatin-refractory metastatic biliary tract cancer, and patients with advanced esophago-gastric cancer who had failed one prior chemotherapy (24–26). On the basis of the positive results of a phase III trial, nal-IRI combination with 5-FU and leucovorin received FDA approval for the treatment of gemcitabine-refractory metastatic pancreatic cancer (27).

[1]Department of Surgery, Indiana University School of Medicine, South Bend, Indiana. [2]Harper Cancer Research Institute, University of Notre Dame, South Bend, Indiana. [3]Department of Pediatrics, Indiana University School of Medicine, South Bend, Indiana. [4]Department of Gastrointestinal Surgery, The Seventh Affiliated Hospital of Sun Yat-sen University, Guangming, Shenzhen, China. [5]Ipsen Bioscience, Cambridge, Massachusetts. [6]Ipsen Innovation, Les Ulis, France. [7]Roswell Park Comprehensive Cancer Center, Buffalo, New York.

Note: Supplementary data for this article are available at Molecular Cancer Therapeutics Online (http://mct.aacrjournals.org/).

Corresponding Author: Niranjan Awasthi, Department of Surgery, Indiana University School of Medicine, 1234 N Notre Dame Avenue, South Bend, IN 46617. Phone: 574-631-5780; E-mail: nawasthi@iu.edu

Mol Cancer Ther 2022;21:1149–59

doi: 10.1158/1535-7163.MCT-21-0860

Tumor angiogenesis plays an integral role in GAC progression and metastasis indicating the potential of antiangiogenic therapy for patients with GAC (28). VEGF and VEGF receptor 2 (VEGFR2)-mediated angiogenesis seem to have an important role in the pathogenesis of GAC, and higher circulating and intratumoral VEGF concentration correlate with tumor aggressiveness and poor survival (29, 30). Ramucirumab, a fully human monoclonal antibody against VEGFR2, received FDA approval as second-line therapy for patients with advanced GAC based on 1.4 months of improvement in median survival compared with placebo (5.2 vs. 3.8 months, HR = 0.776; ref. 31). In another phase III trial with patients with advanced GAC who progressed after first-line chemotherapy with platinum and fluoropyrimidine, ramucirumab plus paclitaxel received FDA approval after exhibiting median survival of 9.6 months compared with 7.4 months with placebo plus paclitaxel (HR = 0.807; ref. 32). DC101 is a murine version of ramucirumab. Cabozantinib, an approved therapy for the treatment of metastatic medullary thyroid cancer, renal cell carcinoma and hepatocellular carcinoma, is a potent small-molecule inhibitor of VEGFR2 that also inhibits c-MET, RET, KIT, and AXL (33). Cabozantinib has been shown to reduce tumor angiogenesis and metastasis in several cancers with dysregulated MET and VEGFR signaling (34). In addition to VEGF, several growth factors and their receptors including PDGF/PDGFR, FGF/FGFR and HGF/HGFR are overexpressed and have all been correlated with poor prognosis in human GAC. Nintedanib (Nin) is a potent triple angiokinase inhibitor of VEGFR1/2/3, FGFR1/2/3 and PDGFRα/β with additional activity against FLT3, Lck, Lyn, and Src (35). Nintedanib has shown antitumor activity in several animal studies and is currently an approved treatment in combination with docetaxel for non–small cell lung cancer in Europe. Nintedanib is currently under clinical investigation in several solid tumors.

The antiangiogenic drugs have limited efficacy as monotherapy and evidence suggests that these drugs enhance the activity of chemotherapy by vascular remodeling, lowering interstitial pressure, increasing blood flow, and possibly by directly impacting tumor cells (36). Because topoisomerase I inhibitor irinotecan has shown activity in gastric cancer, we determined the combination treatment benefits of irinotecan with mechanistically different antiangiogenic drugs. A previous study demonstrated that the combination of bevacizumab, an anti-VEGF antibody, with irinotecan and 5-FU has significant antitumor activity in metastatic colorectal cancer (37). Recently, a phase II trial of ramucirumab plus irinotecan has shown encouraging results as second-line therapy in gastric cancer (38).

In this preclinical study, we tested the hypothesis that nal-IRI has greater antitumor efficacy in mouse models of GAC in comparison with IRI, and the antitumor benefits of nal-IRI can be further improved by the addition of mechanistically different antiangiogenic agents including ramucirumab (or its murine version DC101), cabozantinib or nintedanib.

Materials and Methods

Cell culture and reagents

The human GAC cell lines KATO-III and SNU-5 were purchased from ATCC. The human GAC cell line MKN-45 was purchased from Creative Bioarray. Cells were cultured in RPMI1640 medium (Sigma Chemical Co.) containing 10% or 20% FBS and maintained at 37°C in a humidified incubator with 5% CO_2 and 95% air. Cell lines were authenticated by ATCC (KATO-III, SNU-5) or Creative Bioarray (MKN-45) and were routinely screened to ensure the absence of *Mycoplasma* contamination (InvivoGen). The characteristics of these GAC cell lines are presented in Supplementary Fig. S1. Nal-IRI was obtained from Merrimack Pharmaceuticals. Irinotecan and ramucirumab were purchased from the Goshen Center for Cancer Care pharmacy. DC101 was purchased from BioXcell. Cabozantinib and nintedanib were purchased from LC Labs. SN-38 was purchased from Sigma-Aldrich. The main molecular targets of antiangiogenic agents used in the study are represented in Supplementary Table 1.

Cell proliferation assay

In vitro cell proliferation assays were performed using the colorimetric WST-1 reagent (Sigma). Briefly, 4,000 GAC cells were plated per well in a 96-well plate in the regular growth medium. After 16 hours, the medium was replaced with 2% FBS-containing medium and the cells were treated with SN-38, ramucirumab or nintedanib. After 72 hours incubation, 10 μL WST-1 reagent was added in each well followed by additional incubation for 2 hours. The absorbance was measured at 450 nm using a microplate reader.

Animal studies

All animal studies and procedures were conducted in accordance with the Institutional Animal Care and Use Committee (IACUC) guidelines of the Indiana University School of Medicine (South Bend, IN).

For animal survival studies, 6- to 8-week-old female NOD/SCID mice were purchased from Charles River Laboratories and allowed to acclimate for 1 week before the start of the experiment. Survival studies were performed in a peritoneal dissemination model as previously described (39). Briefly, mice were intraperitoneally injected with 1×10^7 MKN-45 or KATO-III cells. Ten days after tumor cell injection, mice were randomized ($n = 6$–8) into different groups to receive PBS (control), nal-IRI (10 mg/kg, 1×/week), IRI (50 mg/kg, 1×/week), DC101 (40 mg/kg, 2×/week), cabozantinib (30 mg/kg, 5×/week), and nintedanib (25 mg/kg, 5×/week), either as monotherapy or as a combination of nal-IRI or IRI plus antiangiogenic agent, via intraperitoneal injection for 15 days. The doses of nal-IRI, IRI, and antiangiogenic agents were selected on the basis of their clinically equivalent, safe and effective dose range described in the literature (21, 35, 40–42). The experimental procedure of animal survival studies has been presented in Supplementary Fig. S2. Animals were monitored daily and euthanized when moribund according to predefined criteria, including sudden weight gain or loss (>15%), lethargy, inability to remain upright, and lack of strength. Survival was evaluated from the first day of therapy until death as described previously.

For tumor growth studies, MKN-45 cells (7.5×10^6) were subcutaneously implanted into the right flank region of NOD/SCID mice. Ten days after tumor cell injection, mice were randomized ($n = 5$–6) into different groups to receive PBS (control), nal-IRI (10 mg/kg, 1×/week), IRI (50 mg/kg, 1×/week), DC101 (40 mg/kg, 2×/week), or nintedanib (25 mg/kg, 5×/week), either as monotherapy or as a combination of nal-IRI or IRI plus antiangiogenic agent, via intraperitoneal injection for 2 weeks. The tumor size was measured twice weekly, and tumor volume (V) was calculated as $V = {}^1/_2$ (Length × Width^2). Mice were euthanized after completion of therapy, and tumors were dissected and processed for histologic, IHC, and Western blot analysis.

IHC and immunofluorescence

Tumor tissues obtained from subcutaneous xenografts were fixed in 4% paraformaldehyde, dehydrated in a graded series of ethanol, embedded in paraffin, and sectioned. The tumor sections (5 μm) were

deparaffinized with xylene and rehydrated through graded ethanol followed by heat-mediated antigen retrieval using citrate buffer. The tumor sections were incubated for 20 minutes in CAS blocking buffer followed by overnight incubation at 4°C with 1:200 dilution of primary antibodies against Ki67 (Abcam catalog no. ab15580, RRID:AB_443209) or endomucin (rat monoclonal; Millipore Sigma, MAB2624). The tumor sections were washed with PBS and incubated with 1:200 dilution of secondary antibody conjugated with Cy3 (Jackson ImmunoResearch Laboratories) or Alexa Fluor 488 (Life Technologies) at room temperature for 40 minutes to visualize the antigen. Tissues were then washed and mounted with a solution containing 4′,6-diamidino-2-phenylindole (DAPI; Invitrogen) to visualize nuclei. Fluorescence microscopy was used to detect fluorescent signals in five representative high-power field (HPF) per sample using IX81 Olympus microscope and images were captured with a Hamamatsu Orca digital camera (Hamamatsu Corporation) with a DSU spinning confocal unit using CellSens Dimension software (Olympus).

PK evaluation of nal-IRI and IRI

Human GAC MKN-45 cells (6×10^6) were subcutaneously injected into NOD/SCID mice. Ten days after tumor cell injection, animals with measurable tumor were randomized ($n = 20$/group) and treated with nal-IRI or IRI alone or in combination with DC101 or nintedanib as previously described. The experimental procedure of PK evaluation has been presented in Supplementary Fig. S3. After the first dose of nal-IRI or IRI, the first collections were performed after 1, 8, and 24 hours for blood and after 24 hours for tumor, labeled as cohort 1 (C1; 5 mice/group). Second tumor and blood collections were performed at the end of the 3-week therapy (cohort 2, C2; trough level without any additional dosing; 5 mice/group). After the 3-week therapy, an additional PK dose of nal-IRI and IRI was given to the remaining 10 mice of each group, and mouse blood samples were collected at 0.5, 1, 4, 24, 48, and 72 hours after drug treatments using the facial vein technique. Blood sampling was appropriately staggered between the two respective tumor harvest cohorts [5 mice in each group were used for serial blood collection at 0.5, 4, 24 hours and tumor harvest at 24 hours (cohort 3, C3); the remaining mice in each group were used for serial blood collection at 1, 48, 72 hours and tumor harvest at 72 hours (cohort 4, C4)]. Plasma was separated from blood samples, stored at −80°C until analysis for CPT-11 and SN-38 quantification. For tumor analysis, mice were euthanized and perfused with 10 mL PBS, and tumors were harvested, snap-frozen, stored at −80°C until analysis for CPT-11 and SN-38 quantification.

Plasma and tumor levels for CPT-11 and SN-38 were determined using an exploratory LC-triple quadrupole mass spectrometry method. Protein precipitation with a mixture of 25 μL of acetic acid (5% w/v) and 150 μL of methanol containing internal standard (Octreotide) was used for plasma sample pretreatment. Tumor samples were homogenized in methanol using a tissue homogenizer, centrifuged and supernatants were precipitated with methanol containing IS and centrifuged. Finally, the resulting supernatants were placed in a deep well plate containing 20 mmol/L ammonium acetate and 5 μL of each sample, standards, and quality controls for both CPT-11 and SN-38 were injected into the UPLC-MS/MS system (Nexera 2, Shimadzu/API4000, SCIEX) for chromatographic separation on C18 reversed-phase column (2.1×100 mm 1.7 μm Synergi, Phenomenex) and detection in the positive ion electrospray ionization mode. The peak area of the m/z 587.3 to >124.2 and 587.2 to >167.2 transitions of CPT-11, of the m/z 393.2 to >348.7 transition of SN-38 and that of the m/z 510.4 to >120.1 transition of the IS were measured with lower and upper limits of quantification ranging from 0.5 to 5 ng/mL and from 1,000 to 5,000 ng/mL, respectively. For some measurements, an alternative HPLC method described in ref. 22 was employed.

Statistical analysis

Survival study statistics were performed by nonparametric testing with log-rank group comparisons using GraphPad Prism (GraphPad Prism, RRID:SCR_002798). Statistical analysis for *in vivo* tumor growth studies was performed by one-way ANOVA for multiple group comparisons and Student *t* test for the individual group comparisons. Statistical analyses of PK studies were performed using t-test or Wilcoxon–Mann–Whitney test. *In vitro* cell proliferation data are expressed as the mean ± SD; differences were analyzed by two-tailed Student *t* test for the individual group comparison. *P* values of <0.05 were considered to represent statistically significant group differences.

Data availability statement

The data generated in this study are available within the article and its Supplementary Data files.

Results

Nal-IRI increased animal survival more than IRI, combinations with antiangiogenic agents extended survival benefits

In the MKN-45 cell-derived peritoneal dissemination model, the median survival of mice in the control group (PBS treated) was 18 days. At the time of death, control mice had tumors around parts of the stomach including the gastroesophageal junction and at the small bowel, and metastasis was found at the liver, peritoneum, lungs and spleen. Compared with controls, animal survival was increased with antiangiogenic monotherapy: DC101 (21 days, a 17% increase, ns), cabozantinib (24 days, a 33% increase, $P = 0.0009$), and nintedanib (27 days, a 50% increase, $P = 0.0004$). Animal survival was significantly increased by IRI (35 days, a 94% increase, $P = 0.0002$) that was further increased by the addition of antiangiogenic agents: IRI plus DC101 (46 days, a 156% increase, $P = 0.0002$), IRI plus cabozantinib (43 days, a 139% increase, $P = 0.0002$) and IRI+Nin (48 days, a 167% increase, $P = 0.0002$). Importantly, nal-IRI, at one-fifth of the active agent dose compared with IRI, led to a significant improvement in animal survival (46 days, a 156% increase, $P = 0.0002$) that was 31% longer than IRI. Combination of antiangiogenic agents further extended nal-IRI survival benefits: nal-IRI plus DC101 (53 days, a 194% increase, $P = 0.0002$), nal-IRI plus cabozantinib (50 days, a 178% increase, $P = 0.0002$) and nal-IRI plus Nin (52 days, a 189% increase, $P = 0.0002$; **Fig. 1A**).

In KATO-III cell–derived peritoneal dissemination xenografts that carry *FGFR2* gene amplification, the median survival of mice in the control group (PBS treated) was 34 days. Compared with controls, animal survival was notably enhanced by single-agent nal-IRI (259 days, a 662% increase, $P = 0.002$), IRI (199 days, a 485% increase, $P = 0.002$), DC101 (84 days, a 147% increase, $P = 0.002$), and nintedanib (140 days, a 312% increase, $P = 0.002$). Despite the long follow up after a 15-day treatment, a trend of further increase in median survival was observed by the addition of antiangiogenic agents to nal-IRI or IRI therapy groups: nal-IRI plus DC101 (268 days, a 688% increase, $P = 0.002$), nal-IRI plus nintedanib (288 days, a 747% increase, $P = 0.002$), IRI plus DC101 (280 days, a 724% increase, $P = 0.002$), and IRI plus nintedanib (230 days, a 576% increase, $P = 0.002$; **Fig. 1B**).

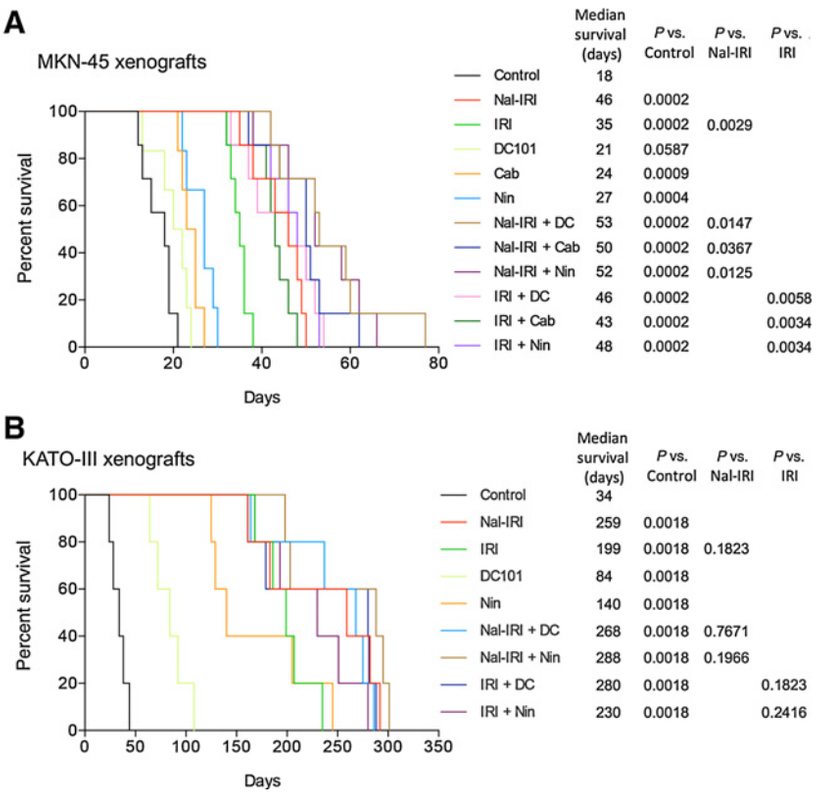

Figure 1.
Animal survival benefits of nal-IRI and improvement in its response by the addition of antiangiogenic agents. Animal survival analysis in (**A**) MKN-45 ($n = 7$) and (**B**) KATO-III ($n = 5$) cell-derived peritoneal dissemination xenografts. Ten days after tumor cell injection, mice were treated with nal-IRI, IRI, DC101, cabozantinib (only in **A**) or nintedanib for 2 weeks. The curve represents the animal survival time from the start of therapy. Statistical group differences in survival time were calculated using log-rank test.

Liposomal irinotecan reduced tumor growth more than IRI, and antiangiogenic agents tend to improve this response, although not statistically significant

In MKN-45 cell–derived subcutaneous xenografts, antiangiogenic monotherapy or chemotherapy (nal-IRI and IRI) resulted in marked tumor growth inhibition, while combinations of nal-IRI or IRI with antiangiogenic agents displayed a trend of additive responses (**Fig. 2A**). The net increase in tumor growth in the control group was 600 mm^3 and compared to controls, tumor growth inhibition was more profound after nal-IRI (92%) than IRI (71%). Tumor growth inhibition was 55% by single-agent DC101 and 71% by single-agent nintedanib. The addition of DC101 or nintedanib enhanced tumor growth inhibition effects to >99% for nal-IRI and >90% for IRI but these additive benefits were not significantly different than their corresponding single-agent chemotherapies (**Fig. 2A**). Final tumor weight data at the end of the treatment period corresponded with tumor growth inhibition data. The mean tumor weight in the control group was 0.81 g. Although the mean tumor weight after nal-IRI therapy (0.23 g) was 39% lower than IRI (0.38 g), this difference was not statistically significant. Again, the addition of antiangiogenic agents DC101 or nintedanib demonstrated a trend of further decrease in tumor weight but these differences were not statistically significant from their corresponding chemotherapy treatments (**Fig. 2B**). During the 2-week treatment phase, there was no apparent treatment-related toxicity and no significant change in mouse body weight in all treatment groups (Supplementary Fig. S4).

Impact of nal-IRI, IRI, and antiangiogenic agents on tumor cell proliferation and vasculature

Examination of tumor cell proliferation by Ki67 immunostaining within tumor tissues obtained from MKN-45 cell-derived subcutaneous xenografts demonstrated that compared with controls (proliferative index 0.81), nal-IRI monotherapy was most effective in reducing intratumoral proliferation (by 58%), followed by IRI (39%), nintedanib (33%), and DC101 (25%). Combinations of nal-IRI with DC101 (61% reduction) or nintedanib (78% reduction) were more effective than single-agent therapies (**Fig. 3**). Combinations of IRI with DC101 (58% reduction) and nintedanib (69% reduction) also had an additive effect in reducing tumor cell proliferation (**Fig. 3**).

Evaluation of microvessel density (MVD) by endomucin immunostaining (43) in tumor tissues obtained from MKN-45 cell–derived subcutaneous xenografts revealed that compared with controls, nal-IRI and IRI had no significant impact on tumor vasculature and the reduction in mean MVD was less than 15%. Compared with controls, mean MVD was significantly reduced by DC101 (57.7%) or nintedanib (65.4%). Microvessel counts in combinations of nal-IRI or IRI with antiangiogenic agents were not different than after antiangiogenic monotherapy (**Fig. 4**).

PK analysis in MKN-45 tumors

PK analysis in MKN-45 cell–derived xenografts after 3 weeks of treatment and one additional PK dose demonstrated that intraperitoneal delivery of nal-IRI resulted in prolonged exposure for both CPT-11 and SN-38 in both plasma and tumor compared with IRI. Plasma levels of SN-38 remained higher for a longer time compared with IRI treatment groups; SN-38 levels were not detected after 4 hours in the IRI treatment groups (**Fig. 5A** and **B**). The addition of DC101 to the nal-IRI treatment did not affect the plasma levels measured for SN-38 and CPT-11 at 4 and 24 hours, however, plasma levels of CPT-11 were lower in the presence of nintedanib and consequently affected SN-38 levels as well (**Fig. 5A** and **B**). Furthermore, after 3 weeks of treatment and before additional PK dose (trough level, C3 predose),

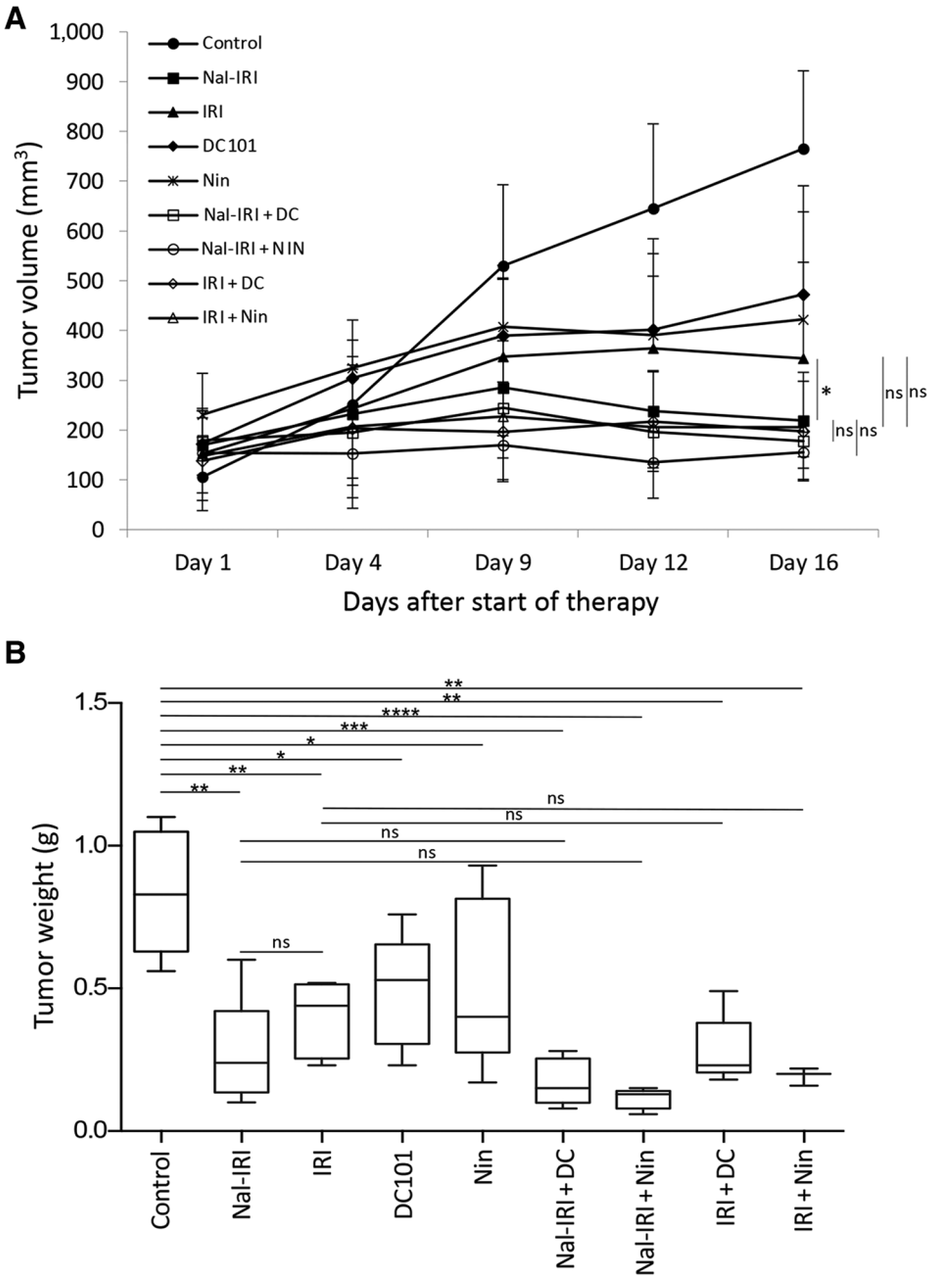

Figure 2.

Reduction in tumor growth by nal-IRI and impact of the addition of antiangiogenic agents. In MKN-45 cell-derived subcutaneous xenografts, ten days after tumor cell injection, mice were treated with nal-IRI, IRI, DC101 and nintedanib for 2 weeks. **A,** Tumor size was measured twice a week during the therapy period using calipers and plotted. Net growth in tumor size was calculated by subtracting tumor volume on the first treatment day from that on the final day. **B,** On the final therapy day, tumors were excised, weighed, and mean tumor weight was calculated in each group and presented as a Box plot. *, $P < 0.05$; **, $P < 0.01$; ***, $P < 0.001$; ****, $P < 0.0001$ by *t* test. Data are representative of mean values ± SD from at least 5 mice per group. Statistical analysis was performed by one-way ANOVA for multiple group comparison and Student *t* test for the individual group comparison.

SN-38 and CPT-11 were undetectable in plasma. However, 24 hours after the additional PK dose, significantly more circulating CPT-11 was detected in nal-IRI compared with IRI treatment groups; CPT-11 plasma level was unchanged after nal-IRI plus DC101, while it decreased after nal-IRI plus nintedanib treatment both at 24 hours after the initial dose and the additional PK dose (**Fig. 5C**). After 3 weeks of IRI treatment and one additional PK dose, some circulating CPT-11 was detected in combination with DC101 and nintedanib 24 hours after dosing (**Fig. 5D**).

Higher intratumoral levels of SN-38 and CPT-11 were detected 24 hours after the additional PK dose (C3) in nal-IRI compared with IRI treatment groups. In this setting, the addition of DC101 to nal-IRI resulted in comparable CPT-11 levels, but nintedanib in combination demonstrated, as observed in plasma, slightly diminished levels. This was not observed with IRI combination (**Fig. 5E** and **F**). SN-38 levels were almost 100-fold higher in nal-IRI and nal-IRI + DC101 at 24 hours after the additional PK dose (C3) compared with 24 hours after the initial dose (C1; **Fig. 5E**). Conversely, for combination with nintedanib, intratumoral SN-38 levels at 24 hours were elevated with both nal-IRI and IRI and similar after the initial dose and the additional PK dose (**Fig. 5F**). After 3 weeks of treatment and one additional PK dose, increased levels of SN-38 and CPT-11 were detected within tumor tissue 24 and 72 hours after nal-IRI treatment compared with IRI treatment groups, and both DC101 and nintedanib combinations led to decreased levels of SN-38 and CPT-11 after 72 hours compared with nal-IRI (**Fig. 5G** and **H**). In addition,

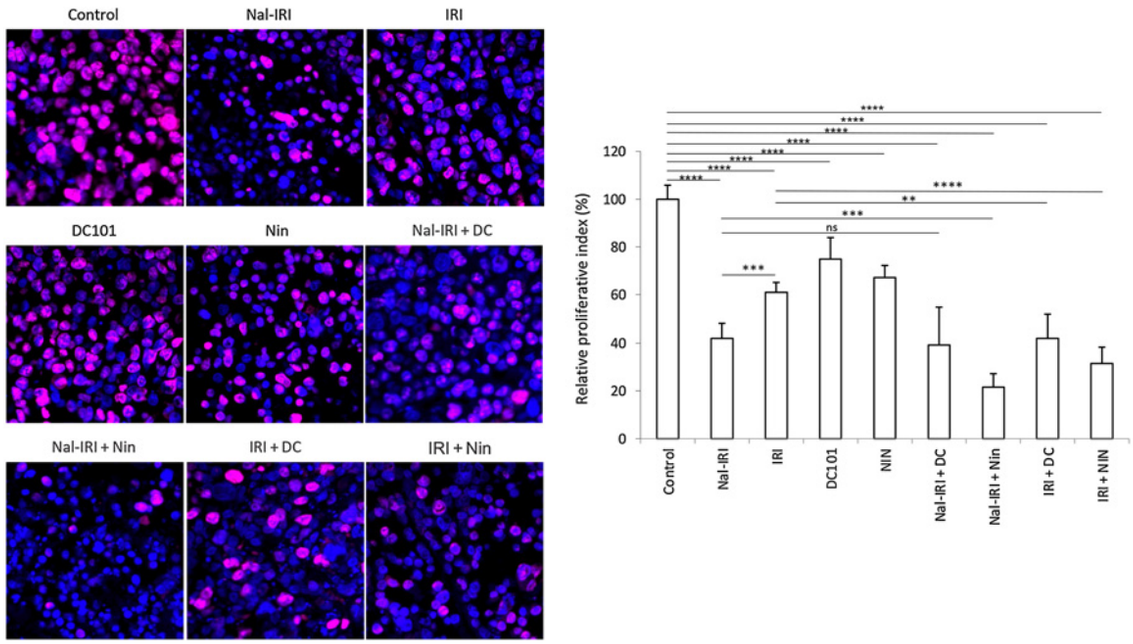

Figure 3.

Effect of nal-IRI and its combination with antiangiogenic agents on tumor cell proliferation. Tumor sections obtained from the MKN-45 subcutaneous xenograft study after 2-week treatment with nal-IRI, IRI, DC101, and nintedanib, were used for the IHC analysis. Tissue sections were immunostained with Ki67 antibody and photographed under a fluorescent microscope. Ki67-positive cells were counted in five different high-power fields. The left panels demonstrate merged images of cell nuclei stained with Ki67 (red) and DAPI (blue) illustrated at 20× magnification. **, $P < 0.01$; ***, $P < 0.001$; ****, $P < 0.0001$ by *t* test. The data are expressed as the mean ± SD.

noticeable predose levels for CPT-11 were observed with either formulation (**Fig. 5H**).

SN-38, IRI, and antiangiogenic agents: effects on *in vitro* GAC cell proliferation

SN-38, the active metabolite of liposomal irinotecan, demonstrated a dose-dependent cell proliferation inhibitory effect on all three cell lines tested. Inhibition of cell proliferation by SN-38 at 100 nmol/L and 10 μmol/L concentrations was 43.3% and 83.4% for MKN-45, 31.7% and 65.6% for KATO-III, and 51.1% versus 84.8% for SNU-5 cells, respectively (**Fig. 6**). Compared with SN-38, the effects of irinotecan, whose conversion is dependent on cellular carboxylesterase activity, were less pronounced on GAC cell lines. Cell proliferation was reduced by IRI at 100 nmol/L and 10 μmol/L concentrations by 0.5% and 8.4% (MKN-45), 14.1% and 26.8% (KATO-III), or 8.5% and 44.1% (SNU-5; **Fig. 6**). Antiangiogenic agents ramucirumab and nintedanib had limited effects at low doses but led to a significant inhibition in cell viability at the higher dose level. A combination of SN-38 or IRI with antiangiogenic agents demonstrated further increased inhibition of GAC cell proliferation (**Fig. 6**).

Discussion

Limited clinical response, high toxicity, and swift development of chemoresistance are common phenomena with currently used standard combination chemotherapy regimens for GAC. Therefore, the search for novel therapeutic strategies with improved clinical efficacy and safety profile is ongoing for this disease. Long-circulating liposomal and nanoparticle formulations of conventional chemotherapy drugs, after intravenous delivery, have several possible advantages including higher permeability, retention, tumor penetration and intratumoral drug concentration levels with the potential for a better safety profile. On the basis of the antitumor efficacy of IRI in GAC and the disadvantages associated with its clinical use, we explored the effects and mechanism of liposomal formulation of irinotecan in GAC preclinical models.

Liposomal irinotecan was developed to overcome the pharmacological and clinical limitations of conventional irinotecan. In this study, we confirmed the PK advantage of nal-IRI resulting in extended plasma and tumor exposure compared with IRI. We observed significantly higher antitumor activity of nal-IRI compared with IRI in several preclinical models of GAC in settings of peritoneal dissemination survival and subcutaneous tumor growth inhibition models. The superior activity of nal-IRI in the peritoneal dissemination xenograft models that bear a close resemblance with the clinical GAC progression pattern is very compelling as peritoneal dissemination is one of the main characteristics of extra-regional metastatic progression of GAC leading to poor prognosis (44). Among the two peritoneal dissemination survival models using human GAC MKN-45 and KATO-III cells, KATO-III xenografts displayed greater chemosensitivity and susceptibility to antiangiogenic treatments, although in the more resistant MKN-45 xenografts the response to nal-IRI was more pronounced relative to IRI. In MKN-45 xenografts, animal survival by nal-IRI was significantly higher than IRI and combinations of nal-IRI with antiangiogenic agents exhibited significant extension in animal survival compared with single-agent therapy. In KATO-III xenografts, nal-IRI showed higher animal survival benefit compared with IRI. The addition of antiangiogenic agents displayed a trend of increase in

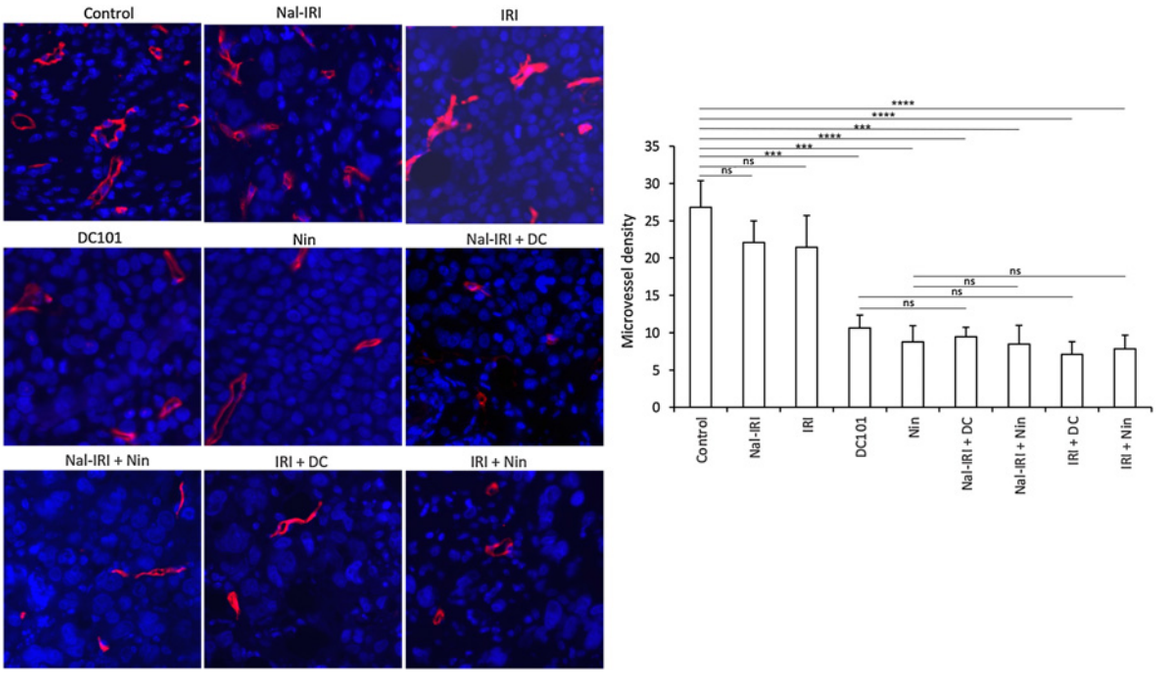

Figure 4.

Effect of nal-IRI and its combination with antiangiogenic agents on microvessel density. Tumor sections obtained from the MKN-45 subcutaneous xenograft study after 2-week treatment were used for evaluating intratumoral microvessel density. Tumor sections were stained with anti-endomucin antibody and slides were photographed under a fluorescent microscope. Endomucin-positive vessels were counted within five different HPF in a blinded manner. The left panels demonstrate merged images of endomucin-positive microvessel (red) and cell nuclei (DAPI, blue) illustrated at 20× magnification. ***, $P < 0.001$; ****, $P < 0.0001$ by *t* test. The data are expressed as the mean ± SD.

animal survival, although not significant probably due to extended survival time beyond completion of therapy and small animal number per group ($n = 5$) in this experiment. The difference in chemosensitivity between MKN-45 and KATO-III xenografts can likely be attributed to differences in oncogenic driver mutations such as *c-met, p53, FGFR2/K-sam*, the expression pattern of oncogenic proteins such as FGFR2, and the differential expression of EMT- and stromal marker proteins in the associated tumor microenvironment (45–47). However, the relative enhancement of nal-IRI effects in the more challenging survival model appears particularly promising for clinical application benefits where extended control is rarely accomplished after conventional cytotoxic agent therapy.

PK measurements indicated that compared with IRI, corroborating with its higher antitumor efficacy, nal-IRI increased the residence time and tumor levels of CPT-11 and its active metabolite SN-38 even after intraperitoneal delivery. These findings were consistent with a previous report in pediatric solid tumor xenografts where nal-IRI treatment demonstrated higher plasma and tumor concentrations of CPT-11 and SN-38 compared with IRI treatment (48). Higher tumor concentrations, as well as longer residence time of CPT-11 and SN-38 after nal-IRI treatment, may be in part accredited to the preferential deposition of liposomes in the tumor lesion due to the EPR effect, followed by liposomal uptake by macrophages in the tumor microenvironment, payload release and concomitant conversion to SN-38 (21, 49). Tumor levels of CPT-11 and SN-38 observed in our PK study after dosing with liposomal irinotecan were within clinically achievable range. Ramanathan and colleagues reported levels of irinotecan and SN-38 averaging 3.73 mcg/g (0.13–12.75 mcg/g) and 14.67 ng/g (1.2–64.0 ng/g), respectively, at 72 hours in patient tumor biopsies (50).

Recent advancement in the molecular profiling of GAC has indicated several actionable oncogenic target mechanisms including *HER2* amplification, mesenchymal-to-epithelial transition, high microsatellite instability, and angiogenesis (51). Tumor angiogenesis plays a critical role in GAC growth, invasion and metastatic dissemination, and several growth factors, their receptors as well as cytokines have been identified to contribute to this process (28). The approval of the HER-2 inhibitor trastuzumab and the VEGFR2 inhibitor ramucirumab further established the potential of growth-inhibitory and antiangiogenic mediators for advancing GAC therapy. In subcutaneous xenografts, DC101, a single target VEGFR2 inhibitor, and nintedanib, a triple angiokinase inhibitor, both exhibited antitumor response in terms of inhibiting tumor growth inhibition, tumor cell proliferation, and MVD. Nal-IRI and IRI had no effect on MVD, and the addition of DC101 or nintedanib to nal-IRI or IRI had no additive benefit on MVD inhibition. In terms of overall tumor growth and tumor cell proliferation, the combination of antiangiogenic agents with nal-IRI or IRI showed a trend to additive inhibitory response, but differences were not statistically significant compared with single-agent therapies. This is probably due to the significantly greater activity of single-agent nal-IRI treatment and changes in the tumor microenvironment by nal-IRI in these settings. Furthermore, among the antiangiogenic agents tested, nintedanib with nal-IRI tend to be more effective in improving animal survival and tumor growth inhibition response based on its higher impact on reducing tumor vasculature and tumor cell proliferation. Greater antitumor activity of nintedanib compared with

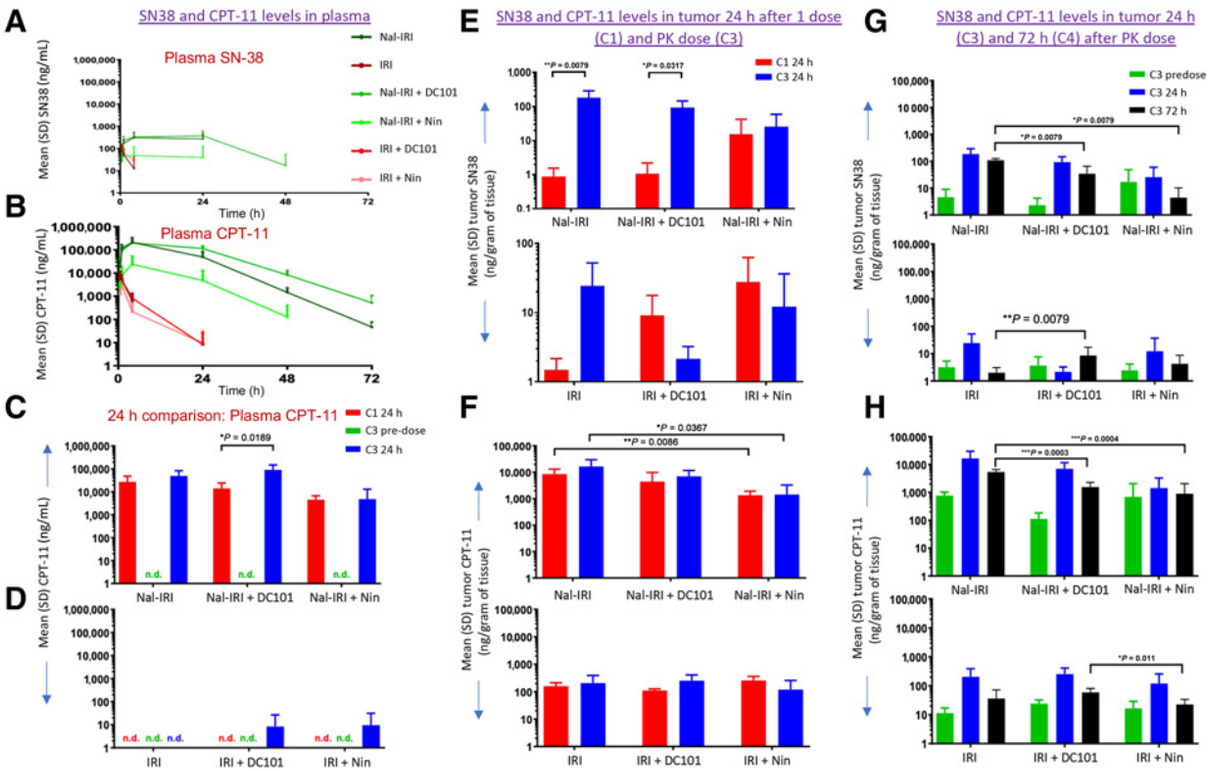

Figure 5.

PK analysis in MKN-45 tumors after nal-IRI, IRI and antiangiogenic therapy. Mice bearing MKN-45 cell–derived xenografts were treated for 3 weeks with nal-IRI, IRI, DC101, and nintedanib. After the first dose of nal-IRI or IRI, the first collections were performed after 1, 8, and 24 hours for plasma and 24 hours for tumor (C1). Additional tumor and plasma collections were performed at the end of the 3-week therapy (C2). After 3-week therapy, a PK dose of nal-IRI and IRI was given to the remaining 10 mice of each group, and mice blood samples were collected at 30 minutes, 1, 4, 24 hours (C3), 48, and 72 hours (C4). **A** and **B,** SN-38 and CPT-11 levels in plasma after a PK dose. **C** and **D,** Comparison of SN-38 and CPT-11 levels 24 hours after the initial dose of nal-IRI and IRI, and 24 hours after the PK dose. For tumor PK analysis, at 0-, 24- (C3), and 72-hour (C4) time points, tumors harvested, and CPT-11 and SN-38 levels were analyzed. **E** and **F,** SN-38 and CPT-11 levels in tumors 24 hours after the initial dose (C1) and PK dose (C3). **G** and **H,** Comparison of SN-38 and CPT-11 levels in tumors 24 (C3) and 72 hours (C4) after PK dose.

DC101 may also be related to multikinase inhibitory action of nintedanib blocking multiple angiogenic signaling pathways including VEGF/VEGFR, FGF/FGFR and PDGF/PDGFR, in addition to other off-target effects, rather than the single-target murine VEGFR2 signaling inhibition of DC101. Thus, the differential antitumor benefits of antiangiogenic drugs in this study can likely be in part accredited to their target specificity, and a resulting capability of nintedanib to directly impact both (human) tumor epithelial and (murine) stromal and endothelial compartments (52, 53).

Vessel normalization by antiangiogenic drugs is thought to improve the availability of small-molecule drugs in tumor lesions. However, for larger particles such as liposomal formulation the delivery may depend on their size and other lesion characteristics (54–56). In this study, the addition of nintedanib or DC101 to IRI therapies led to increased antitumor responses over the cytotoxic agents alone. However, when comparing drug levels across treatment cycles or for combinations against the monotherapy, no strong differences were observed for DC101 for either the IRI or nal-IRI formulations, although a trend toward lower average deposition was suggested for the liposomal formulation (**Fig. 5F**). Cytotoxic treatment alone with or without DC101 irrespective of the formulation consistently, but minimally, increased CPT-11 levels after the third dosing cycle compared to the first dosing cycle. It also appeared to increase local conversion to or reduced clearance of SN-38 at the later timepoint suggesting dynamic changes due to anti-tumor efficacy alone. In contrast, the addition of nintedanib to nal-IRI therapy affected the systemic availability of the liposome resulting in lower tumoral drug levels at both initial and late dosing cycles (**Fig. 5E** and **F**) although elevated trough levels for both CPT-11 and SN-38 prior to the additional PK dose were surprisingly maintained (**Fig. 5G** and **H**). It is not clear if this is due to the modus of intraperitoneal delivery and any impact of nintedanib on lymphatic drainage or other effects on tissue distribution. Furthermore, elevated tumoral levels of SN-38 in the presence of nintedanib even after the initial treatment dose seen for both IRI and nal-IRI are reminiscent of effects of TKIs such as lapatinib on ATP binding cassette transporter systems that reduce SN-38 efflux from tumoral cells (57). Thus, any effects of a normalized tumor vasculature on tumoral drug distribution are blurred by direct antitumor treatment effects as well as, possibly, dynamic changes in transporter characteristics, metabolic reprogramming or altered macrophage activity (58–60). Overall, in the present model, it seems that antitumor mechanisms of the antiangiogenic agents affecting vessel functionality and leading to decreased vessel density as well as direct antitumor cytotoxic

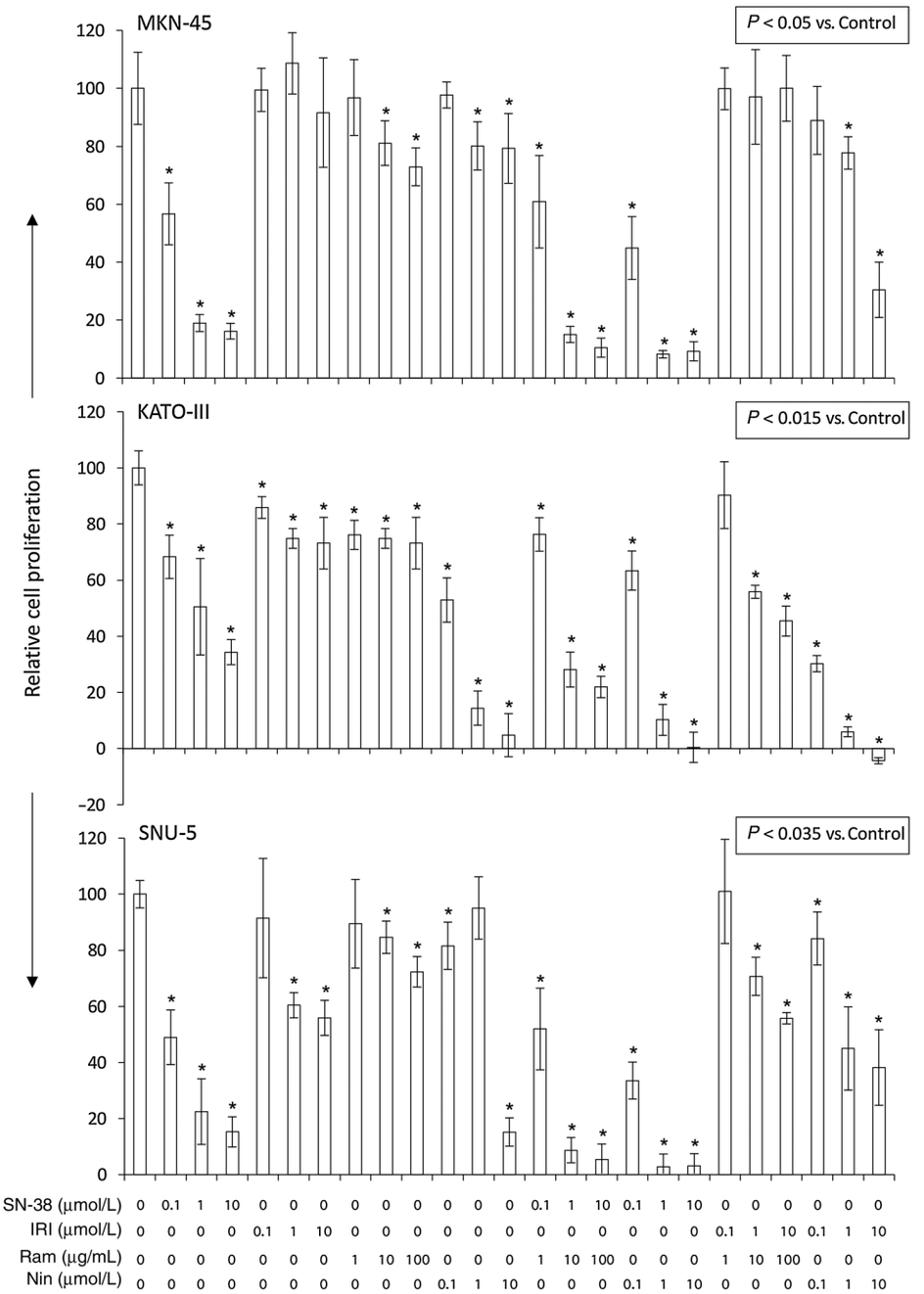

Figure 6.

In vitro cell proliferation inhibition by SN-38 and IRI: impact of the addition of antiangiogenic agents. GAC cells (MKN-45, KATO-III, and SNU-5) were plated on 96-well plates and treated with SN-38, irinotecan, ramucirumab, or nintedanib. After 72-hour incubation, WST-1 reagent (10 μL) was added to each well followed by additional incubation for 2 hours. The absorbance at 450 nm was measured using a microplate reader. The resulting number of viable cells was calculated by measuring the absorbance of color produced in each well. Data are the mean ± SD of triplicate determinations.

activity outweigh their possible protumorigenic effects as a result of, potentially, changes in drug deposition or cytotoxic drug clearance characteristics.

On the basis of highly heterogeneous nature of human cancers, there are limitations of cell line-based animal models due to their clonal nature and adaptations to defined culture media. The clinical development of nal-IRI as monotherapy or in combination with 5-FU containing regimens and other combinations is ongoing with multiple clinical signals being continuously reported across indications. The reported findings continue to build support for a better therapeutic index of the nal-IRI formulation. The present study provides additional insights into tumor deposition characteristics of nal-IRI in the presence of antiangiogenic drugs, how the combination of nal-IRI with antiangiogenic drugs affects the efficacy of nanotherapeutics, and the intraperitoneal accessibility of tumor models to nal-IRI–mediated treatment benefits. This study supports the therapeutic potential of liposomal irinotecan in GAC based on its significantly higher antitumor efficacy compared with irinotecan. Although the observed combination treatment benefits were small, based on the multifactorial angiogenic mechanisms observed in GAC, this study also supports a clinical potential of a combined antiangiogenic approach with nal-IRI, in particular for the triple angiokinase inhibitor nintedanib or other

multitarget TKIs. The therapeutic efficacy of liposomal irinotecan and an improvement in its response by nintedanib as observed may open additional avenues for improved clinical GAC therapy.

Authors' Disclosures

N. Awasthi reports grants and non-financial support from Merrimack Pharmaceuticals and grants and non-financial support from Ipsen Biopharmaceuticals during the conduct of the study; grants from Boehringer Ingelheim Pharmaceuticals outside the submitted work. S.G. Klinz reports personal fees and other support from Ipsen Bioscience outside the submitted work. No disclosures were reported by the other authors. All Ipsen authors should be noted as employees (SG, BB, FM-L and AT at time of the study).

Authors' Contributions

N. Awasthi: Conceptualization, resources, data curation, formal analysis, supervision, funding acquisition, validation, investigation, visualization, methodology, writing–original draft, writing–review and editing. **M.A. Schwarz:** Data curation, methodology. **C. Zhang:** Data curation, methodology. **S.G. Klinz:** Conceptualization, resources, data curation, formal analysis, writing–review and editing. **F. Meyer-Losic:** Data curation, formal analysis, methodology, writing–review and editing. **B. Beaufils:** Data curation, formal analysis, validation, writing–review and editing. **A. Thiagalingam:** Conceptualization, data curation, writing–review and editing. **R.E. Schwarz:** Conceptualization, data curation, supervision, writing–review and editing.

Acknowledgments

This research work was financially supported by Merrimack Pharmaceuticals, Ipsen Biopharmaceuticals, and Indiana University School of Medicine funds (to N. Awasthi and R.E. Schwarz). We thank the members of the MM-398 Research team at Merrimack Pharmaceuticals, especially Helen Lee and Shannon Leonard, for their instrumental contributions to the execution of this project.

The costs of publication of this article were defrayed in part by the payment of page charges. This article must therefore be hereby marked *advertisement* in accordance with 18 U.S.C. Section 1734 solely to indicate this fact.

Received October 26, 2021; revised February 22, 2022; accepted April 28, 2022; published first May 2, 2022.

References

1. Bray F, Ferlay J, Soerjomataram I, Siegel RL, Torre LA, Jemal A. Global cancer statistics 2018: GLOBOCAN estimates of incidence and mortality worldwide for 36 cancers in 185 countries. CA Cancer J Clin 2018;68:394–424.
2. Webb A, Cunningham D, Scarffe JH, Harper P, Norman A, Joffe JK, et al. Randomized trial comparing epirubicin, cisplatin, and fluorouracil versus fluorouracil, doxorubicin, and methotrexate in advanced esophagogastric cancer. J Clin Oncol 1997;15:261–7.
3. Cunningham D, Starling N, Rao S, Iveson T, Nicolson M, Coxon F, et al. Capecitabine and oxaliplatin for advanced esophagogastric cancer. N Engl J Med 2008;358:36–46.
4. Park SR, Chun JH, Kim YW, Lee JH, Choi IJ, Kim CG, et al. Phase II study of low-dose docetaxel/fluorouracil/cisplatin in metastatic gastric carcinoma. Am J Clin Oncol 2005;28:433–8.
5. Al-Batran SE, Hofheinz RD, Pauligk C, Kopp HG, Haag GM, Luley KB, et al. Histopathological regression after neoadjuvant docetaxel, oxaliplatin, fluorouracil, and leucovorin versus epirubicin, cisplatin, and fluorouracil or capecitabine in patients with resectable gastric or gastro-oesophageal junction adenocarcinoma (FLOT4-AIO): results from the phase 2 part of a multicentre, open-label, randomised phase 2/3 trial. Lancet Oncol 2016;17:1697–708.
6. Ghosn M, Tabchi S, Kourie HR, Tehfe M. Metastatic gastric cancer treatment: Second line and beyond. World J Gastroenterol 2016;22:3069–77.
7. Shi WJ, Gao JB. Molecular mechanisms of chemoresistance in gastric cancer. World J Gastrointest Oncol 2016;8:673–81.
8. Hsiang YH, Lihou MG, Liu LF. Arrest of replication forks by drug-stabilized topoisomerase I-DNA cleavable complexes as a mechanism of cell killing by camptothecin. Cancer Res 1989;49:5077–82.
9. Futatsuki K, Wakui A, Nakao I, Sakata Y, Kambe M, Shimada Y, et al. [Late phase II study of irinotecan hydrochloride (CPT-11) in advanced gastric cancer. CPT-11 Gastrointestinal Cancer Study Group]. Gan To Kagaku Ryoho 1994;21:1033–8.
10. Bouche O, Raoul JL, Bonnetain F, Giovannini M, Etienne PL, Lledo G, et al. Randomized multicenter phase II trial of a biweekly regimen of fluorouracil and leucovorin (LV5FU2), LV5FU2 plus cisplatin, or LV5FU2 plus irinotecan in patients with previously untreated metastatic gastric cancer: a Federation Francophone de Cancerologie Digestive Group Study–FFCD 9803. J Clin Oncol 2004;22:4319–28.
11. Ajani JA, Baker J, Pisters PW, Ho L, Mansfield PF, Feig BW, et al. CPT-11 plus cisplatin in patients with advanced, untreated gastric or gastroesophageal junction carcinoma: results of a phase II study. Cancer 2002;94:641–6.
12. Chun JH, Kim HK, Lee JS, Choi JY, Lee HG, Yoon SM, et al. Weekly irinotecan in patients with metastatic gastric cancer failing cisplatin-based chemotherapy. Jpn J Clin Oncol 2004;34:8–13.
13. Kim ST, Kang WK, Kang JH, Park KW, Lee J, Lee SH, et al. Salvage chemotherapy with irinotecan, 5-fluorouracil and leucovorin for taxane- and cisplatin-refractory, metastatic gastric cancer. Br J Cancer 2005;92:1850–4.
14. Kunisaki C, Imada T, Yamada R, Hatori S, Ono H, Otsuka Y, et al. Phase II study of docetaxel plus cisplatin as a second-line combined therapy in patients with advanced gastric carcinoma. Anticancer Res 2005;25:2973–7.
15. Chabot GG. Clinical pharmacokinetics of irinotecan. Clin Pharmacokinet 1997;33:245–59.
16. Messerer CL, Ramsay EC, Waterhouse D, Ng R, Simms EM, Harasym N, et al. Liposomal irinotecan: formulation development and therapeutic assessment in murine xenograft models of colorectal cancer. Clin Cancer Res 2004;10:6638–49.
17. Stewart CF, Zamboni WC, Crom WR, Houghton PJ. Disposition of irinotecan and SN-38 following oral and intravenous irinotecan dosing in mice. Cancer Chemother Pharmacol 1997;40:259–65.
18. Rowinsky EK, Grochow LB, Ettinger DS, Sartorius SE, Lubejko BG, Chen TL, et al. Phase I and pharmacological study of the novel topoisomerase I inhibitor 7-ethyl-10-[4-(1-piperidino)-1-piperidino]carbonyloxycamptothecin (CPT-11) administered as a ninety-minute infusion every 3 weeks. Cancer Res 1994;54:427–36.
19. Kehrer DF, Sparreboom A, Verweij J, de Bruijn P, Nierop CA, van de Schraaf J, et al. Modulation of irinotecan-induced diarrhea by cotreatment with neomycin in cancer patients. Clin Cancer Res 2001;7:1136–41.
20. Drummond DC, Noble CO, Guo Z, Hong K, Park JW, Kirpotin DB. Development of a highly active nanoliposomal irinotecan using a novel intraliposomal stabilization strategy. Cancer Res 2006;66:3271–7.
21. Kalra AV, Kim J, Klinz SG, Paz N, Cain J, Drummond DC, et al. Preclinical activity of nanoliposomal irinotecan is governed by tumor deposition and intratumor prodrug conversion. Cancer Res 2014;74:7003–13.
22. Leonard SC, Lee H, Gaddy DF, Klinz SG, Paz N, Kalra AV, et al. Extended topoisomerase 1 inhibition through liposomal irinotecan results in improved efficacy over topotecan and irinotecan in models of small-cell lung cancer. Anticancer Drugs 2017;28:1086–96.
23. Noble CO, Krauze MT, Drummond DC, Forsayeth J, Hayes ME, Beyer J, et al. Pharmacokinetics, tumor accumulation and antitumor activity of nanoliposomal irinotecan following systemic treatment of intracranial tumors. Nanomedicine (Lond) 2014;9:2099–108.
24. Ko AH, Tempero MA, Shan YS, Su WC, Lin YL, Dito E, et al. A multinational phase 2 study of nanoliposomal irinotecan sucrosofate (PEP02, MM-398) for patients with gemcitabine-refractory metastatic pancreatic cancer. Br J Cancer 2013;109:920–5.
25. Yoo C, Kim K-P, Kim I, Kang MJ, Cheon J, Kang BW, et al. Liposomal irinotecan (nal-IRI) in combination with fluorouracil (5-FU) and leucovorin (LV) for patients with metastatic biliary tract cancer (BTC) after progression on gemcitabine plus cisplatin (GemCis): Multicenter comparative randomized phase 2b study (NIFTY). J Clin Oncol 2021;39:4006.
26. Roy AC, Park SR, Cunningham D, Kang YK, Chao Y, Chen LT, et al. A randomized phase II study of PEP02 (MM-398), irinotecan or docetaxel as a second-line therapy in patients with locally advanced or metastatic gastric or gastro-oesophageal junction adenocarcinoma. Ann Oncol 2013;24:1567–73.

27. Wang-Gillam A, Li CP, Bodoky G, Dean A, Shan YS, Jameson G, et al. Nanoliposomal irinotecan with fluorouracil and folinic acid in metastatic pancreatic cancer after previous gemcitabine-based therapy (NAPOLI-1): a global, randomised, open-label, phase 3 trial. Lancet 2016;387:545–57.
28. Hsieh HL, Tsai MM. Tumor progression-dependent angiogenesis in gastric cancer and its potential application. World J Gastrointest Oncol 2019;11: 686–704.
29. Lieto E, Ferraraccio F, Orditura M, Castellano P, Mura AL, Pinto M, et al. Expression of vascular endothelial growth factor (VEGF) and epidermal growth factor receptor (EGFR) is an independent prognostic indicator of worse outcome in gastric cancer patients. Ann Surg Oncol 2008;15:69–79.
30. Murukesh N, Dive C, Jayson GC. Biomarkers of angiogenesis and their role in the development of VEGF inhibitors. Br J Cancer 2010;102:8–18.
31. Fuchs CS, Tomasek J, Yong CJ, Dumitru F, Passalacqua R, Goswami C, et al. Ramucirumab monotherapy for previously treated advanced gastric or gastro-oesophageal junction adenocarcinoma (REGARD): an international, randomised, multicentre, placebo-controlled, phase 3 trial. Lancet 2014;383:31–9.
32. Wilke H, Muro K, Van Cutsem E, Oh SC, Bodoky G, Shimada Y, et al. Ramucirumab plus paclitaxel versus placebo plus paclitaxel in patients with previously treated advanced gastric or gastro-oesophageal junction adenocarcinoma (RAINBOW): a double-blind, randomised phase 3 trial. Lancet Oncol 2014;15:1224–35.
33. Rathi N, Maughan BL, Agarwal N, Swami U. Mini-review: cabozantinib in the treatment of advanced renal cell carcinoma and hepatocellular carcinoma. Cancer Manag Res 2020;12:3741–9.
34. Yakes FM, Chen J, Tan J, Yamaguchi K, Shi Y, Yu P, et al. Cabozantinib (XL184), a novel MET and VEGFR2 inhibitor, simultaneously suppresses metastasis, angiogenesis, and tumor growth. Mol Cancer Ther 2011;10:2298–308.
35. Hilberg F, Roth GJ, Krssak M, Kautschitsch S, Sommergruber W, Tontsch-Grunt U, et al. BIBF 1120: triple angiokinase inhibitor with sustained receptor blockade and good antitumor efficacy. Cancer Res 2008;68:4774–82.
36. Ma J, Waxman DJ. Combination of antiangiogenesis with chemotherapy for more effective cancer treatment. Mol Cancer Ther 2008;7:3670–84.
37. Hurwitz H, Fehrenbacher L, Novotny W, Cartwright T, Hainsworth J, Heim W, et al. Bevacizumab plus irinotecan, fluorouracil, and leucovorin for metastatic colorectal cancer. N Engl J Med 2004;350:2335–42.
38. Kawamoto Y, Yuki S, Sawada K, Nakamura M, Muto O, Sogabe S, et al. Results of a phase II trial of ramucirumab plus irinotecan as second-line treatment for patients with advanced gastric cancer (HGCSG 1603). J Clin Oncol 2021;39:217.
39. Schwarz RE, Awasthi N, Konduri S, Cafasso D, Schwarz MA. EMAP II-based antiangiogenic-antiendothelial in vivo combination therapy of pancreatic cancer. Ann Surg Oncol 2010;17:1442–52.
40. Mohammad AS, Griffith JI, Adkins CE, Shah N, Sechrest E, Dolan EL, et al. Liposomal irinotecan accumulates in metastatic lesions, crosses the blood-tumor barrier (BTB), and prolongs survival in an experimental model of brain metastases of triple negative breast cancer. Pharm Res 2018;35:31.
41. Tonra JR, Corcoran E, Deevi DS, Steiner P, Kearney J, Li H, et al. Prioritization of EGFR/IGF-IR/VEGFR2 combination targeted therapies utilizing cancer models. Anticancer Res 2009;29:1999–2007.
42. Xiang Q, Chen W, Ren M, Wang J, Zhang H, Deng DY, et al. Cabozantinib suppresses tumor growth and metastasis in hepatocellular carcinoma by a dual blockade of VEGFR2 and MET. Clin Cancer Res 2014;20:2959–70.
43. Liu C, Shao ZM, Zhang L, Beatty P, Sartippour M, Lane T, et al. Human endomucin is an endothelial marker. Biochem Biophys Res Commun 2001;288: 129–36.
44. Kanda M, Kodera Y. Molecular mechanisms of peritoneal dissemination in gastric cancer. World J Gastroenterol 2016;22:6829–40.
45. Yokozaki H. Molecular characteristics of eight gastric cancer cell lines established in Japan. Pathol Int 2000;50:767–77.
46. Chen D, Cao G, Qiao C, Liu G, Zhou H, Liu Q. Alpha B-crystallin promotes the invasion and metastasis of gastric cancer via NF-κB-induced epithelial-mesenchymal transition. J Cell Mol Med 2018;22:3215–22.
47. Yuan TM, Liang RY, Hsiao NW, Chuang SM. The S100A4 D10V polymorphism is related to cell migration ability but not drug resistance in gastric cancer cells. Oncol Rep 2014;32:2307–18.
48. Kang MH, Wang J, Makena MR, Lee JS, Paz N, Hall CP, et al. Activity of MM-398, nanoliposomal irinotecan (nal-IRI), in Ewing's family tumor xenografts is associated with high exposure of tumor to drug and high SLFN11 expression. Clin Cancer Res 2015;21:1139–50.
49. Leonard SC, Paz N, Klinz SG, Gaddy D, Lee H, Hendriks BS, et al. Deposition characteristics and resulting DNA damage patterns of liposomal irinotecan (nal-IRI) in pancreatic cancer xenografts. J Clin Oncol 2018;36:335.
50. Ramanathan RK, Korn RL, Sachdev JC, Fetterly GJ, Jameson G, Marceau K, et al. 261 Lesion characterization with ferumoxytol MRI in patients with advanced solid tumors and correlation with treatment response to MM-398, nanoliposomal irinotecan (nal-IRI). Eur J Cancer 2014;50:87.
51. Selim JH, Shaheen S, Sheu WC, Hsueh CT. Targeted and novel therapy in advanced gastric cancer. Exp Hematol Oncol 2019;8:25.
52. Hilberg F, Tontsch-Grunt U, Baum A, Le AT, Doebele RC, Lieb S, et al. Triple angiokinase inhibitor nintedanib directly inhibits tumor cell growth and induces tumor shrinkage via blocking oncogenic receptor tyrosine kinases. J Pharmacol Exp Ther 2018;364:494–503.
53. Kato R, Haratani K, Hayashi H, Sakai K, Sakai H, Kawakami H, et al. Nintedanib promotes antitumour immunity and shows antitumour activity in combination with PD-1 blockade in mice: potential role of cancer-associated fibroblasts. Br J Cancer 2021;124:914–24.
54. Chauhan VP, Stylianopoulos T, Martin JD, Popović Z, Chen O, Kamoun WS, et al. Normalization of tumour blood vessels improves the delivery of nanomedicines in a size-dependent manner. Nat Nanotechnol 2012;7:383–8.
55. Goel S, Duda DG, Xu L, Munn LL, Boucher Y, Fukumura D, et al. Normalization of the vasculature for treatment of cancer and other diseases. Physiol Rev 2011; 91:1071–121.
56. Mattheolabakis G, Mikelis CM. Nanoparticle delivery and tumor vascular normalization: The chicken or the egg? Front Oncol 2019;9:1227.
57. Wu S, Fu L. Tyrosine kinase inhibitors enhanced the efficacy of conventional chemotherapeutic agent in multidrug resistant cancer cells. Mol Cancer 2018; 17:25.
58. Jászai J, Schmidt MHH. Trends and challenges in tumor Anti-angiogenic therapies. Cells 2019;8:1102.
59. Ma S, Pradeep S, Hu W, Zhang D, Coleman R, Sood A. The role of tumor microenvironment in resistance to anti-angiogenic therapy. F1000Res 2018; 7:326.
60. Minchinton AI, Tannock IF. Drug penetration in solid tumours. Nat Rev Cancer 2006;6:583–92.